Synergistic effects of previous winter NAO and ENSO on the spring dust activities in North China

Falei Xu[1], Shuang Wang[1], Yan Li[2], and Juan Feng[1]

[1]State Key Laboratory of Remote Sensing Science, Faculty of Geographical Science, Beijing Normal University, Beijing, China

[2]Key Laboratory for Semi-Arid Climate Change of the Ministry of Education, College of Atmospheric Sciences, Lanzhou University, Lanzhou, China

Correspondence: Juan Feng (fengjuan@bnu.edu.cn)

Abstract

Dust plays an important role in influencing global weather and climate by impacting the Earth's radiative balance. Based on the reanalysis datasets during 1979-2022, the impacts of preceding winter North Atlantic Oscillation (NAO) and El Niño-Southern Oscillation (ENSO) on the following spring dust activities over North China are explored. It is found that both the NAO and ENSO exert significant effects on dust activities in North China, especially during their negative phases. When both of them are in the negative phases, their combined impacts on the dust activities exceeding that of either factor individually. The previous winter NAO exhibits significant impacts on the sea surface temperatures (SST) in the North Atlantic, associated with an anomalous SST tripole pattern. These SST anomalies can persist to the following spring due to their inherent persistence, when anomalous atmospheric teleconnection wave trains would be induced, thereby influencing the dust activities in North China. ENSO, on the one hand, directly impacts dust activities in North China by modulating the circulation in the Western North Pacific (WNP). Additionally, ENSO enhances the NAO's effect on the North Atlantic SST, explaining their synergistic effects on the dust activities over North China. This study elucidates the combined roles of NAO and ENSO on the dust activities over North China, providing one season ahead signals for predicting spring dust activities in North China.

1. Introduction

Dust, as one of the most significant natural aerosols in the atmosphere, is of great importance to the global radiative balance with its light-absorbing properties, exerting a crucial role in climate change (e.g., Lou et al., 2017; Li et al., 2022; Kok et al., 2023). Moreover, dust not only influences its source regions but also extends its impact across oceans via teleconnections driven by atmospheric circulation. This transboundary transport affects ocean-atmosphere interactions and has a profound impact on the Earth's climate system (Huang et al., 2015). Dust activities, resulting from regional dust surges, poses a formidable threat to socio-economic development, natural ecological environment, as well as human health and safety (Zhao et al., 2020; Li et al., 2023). The Gobi Desert in East Asia, particularly the Mongolian Plateau and Northern China, is a major source of dust (Chen et al., 2023; Hu et al., 2023), contributing approximately 70% of Asia's total dust emissions (Zhang et al., 2003). Given that China is one of the countries profoundly impacted by dust activities (Fan et al., 2018), exploring the variations in dust activities in China is of significant scientific and practical importance.

Besides the dust source regions over China (mainly Xinjiang and Inner Mongolia), North China also exhibited high dust content and significant dust interannual variability (Liu et al., 2004; Ji and Fan, 2019). Additionally, as a crucial center of politics, economy, and population, it is meaningful to investigate the variations of spring dust activities over North China (30-40°N, 105-120°E) and explore the relevant physical mechanisms. Previous studies have revealed that the frequency of dust events in China exhibits strong interannual and interdecadal characteristics, with high frequency from the 1950s to 1970s, low frequency from the 1980s to 1990s, and a notable increase after 2000 (Zhu et al., 2008; Ji and Fan, 2019). On interdecadal time scales, climate oscillations such as the Atlantic Multidecadal Oscillation (AMO), Pacific Decadal Oscillation (PDO), as well as Antarctic Oscillation (AAO) can influence the dust activities by affecting the climate background. For instance, the positive phase of PDO is favorable for reduced dust activities by influencing the westerly belt, leading to weaker dust activities (uplift and deposition) in the Asian region (Gong et al., 2006). The AMO plays a role in affecting the global aridification process by altering the thermal properties between land and sea (Huang et al., 2017). Additionally, the AAO may substantially regulate dust activities in China by affecting the frequency of dust in East Asia through the interaction of meridional circulations between the Northern and Southern Hemispheres (Ji and Fan, 2019).

On the interannual scale, a weaker East Asian Winter Monsoon (EAWM) is associated with

anomalous circulation over the Gobi and Taklamakan deserts, facilitating the transport of dust, consequently increasing dust content in China (Lou et al., 2016). The variations of the sea ice coverage in the Barents Sea can significantly influence the intensity and frequency of dust activities in China by affecting cyclone generation and thermal instability in North China (Fan et al., 2018). The North Atlantic Oscillation (NAO) exert a substantial influence on the spring dust activities in North China by modulating the zonal wave train from the Atlantic to the Pacific at mid-latitudes in the Northern Hemisphere, as well as the sea level pressure (SLP) gradient in the Tarim Basin in China (Zhao et al., 2013). On the synoptic scale, the NAO exerts a vital influence on the emergence and evolution of dust activities in North China by impacting the transport of transient wave flux and modifying atmospheric circulation (Li et al., 2023). Beyond extratropical signals, tropical variabilities, such as El Niño–Southern Oscillation (ENSO), also significantly modulated dust activities in China by regulating variations in large-scale circulation, precipitation, and temperature over East Asia (Yang et al., 2022), as well as in Saudi Arabia (Yu et al., 2015), Central Asia (Xi and Sokolik, 2015), and North America (Achakulwisut et al., 2017).

From the aforementioned studies on the dust activities in China, it is evident that the NAO and ENSO are two important factors, with a focus on their individual effects on the dust activities in China. However, as significant climate variabilities in the extratropical and tropical regions, respectively, the NAO and ENSO often co-occur and have complex interactions (López-Parages et al., 2015). It is found that ENSO can influence the climate near the North Atlantic through atmospheric forcing of the Pacific-North America teleconnection (Wallace and Gutzler, 1981). During the early winter of El Niño events, strong convective anomalies in the tropical Indian Ocean-Western Pacific (Abid et al., 2021) and the Gulf of Mexico-Caribbean Sea (Ayarzagüena et al., 2018) can trigger Rossby wave trains reaching the North Atlantic, leading to positive NAO signals, and vice versa. Furthermore, the stratosphere, serving as an energy transmission channel, may also be an important pathway for ENSO to influence the NAO (Jiménez-Esteve and Domeisen, 2018). Moreover, observations and numerical simulations have demonstrated that the NAO signal can induce a Gill-Matsuno pattern in the tropical region of southern Eurasia, inducing a decadal enhancement in the linkage between the East Asian Summer Monsoon (EASM) and ENSO (Wu et al., 2012). When the NAO is in its positive phase, intensified northeasterlies are observed over tropical North Atlantic, resulting in increased low-level moisture content and precipitation in the tropical North Atlantic, paralleling with stronger convection and enhanced ENSO impact (Ding et al., 2023). These studies highlight the connections and interactions between NAO and ENSO, underscoring the necessity of considering their synergistic effects on the dust activities in North

China.

The synergistic effect refers to the phenomenon where the combined impacts of two or more factors are significantly greater than their individual roles (Li et al., 2019). It has been found that there are synergistic effects in the impact of NAO and ENSO on the weather and climate in China. The NAO can facilitate the development of the subpolar teleconnection across northern Eurasia downstream, leading to anomalies in the high-pressure systems over the Ural Mountains and the Sea of Okhotsk, which in turn affect the EASM (Wang et al., 2000). Meanwhile, ENSO exerts significant impact on the convective activities in the central Pacific and induces alterations in the equatorial circulation via the Pacific-East Asia teleconnection, further affecting the atmospheric circulation and sea surface temperature (SST) in the Western North Pacific (WNP), ultimately influencing the intensity of the EASM (Wang et al., 2000). Therefore, the synergistic effects of these factors can result in pronounced impacts on the EASM (Wu et al., 2009). During El Niño events, SST in the central and eastern equatorial Pacific rises, enhancing convective activity near the equator, which brings more moisture to North China and increases the likelihood of precipitation. Simultaneously, the positive phase of NAO can alter atmospheric pressure in the North Atlantic, influencing atmospheric circulation over the Eurasian continent. This interaction between NAO and ENSO synergistically regulates, to some extent, the distribution of precipitation in North China (Guo et al., 2012).

The synergistic effects of NAO and ENSO significantly influence the climate in China, but their synergistic effects on the dust activities over North China and the mechanisms involved remain unclear. This study will investigate these effects on dust activities over North China, providing a scientific foundation for predicting dust activities in China. The structure of this paper is as follows: Section 2 outlines the datasets and methods employed in this study. Section 3 presents the analysis and findings. Section 4 contains the summary and discussion.

2. Datasets and methods

2.1 Datasets

The dust dataset for the Modern-Era Retrospective Analysis for Research and Applications Version 2 (MERRA-2) was obtained from NASA's Global Modeling and Assimilation Office (GMAO), incorporating assimilated observations from both satellites and ground stations (Gelaro et al., 2017). In this study, the Dust Column Mass Density of the MERRA-2 tavg1_2d_aer_Nx product was utilized to represent the dust content with a $0.5° \times 0.625°$ resolution. Previous studies

have demonstrated the applicability of MERRA-2 reanalysis data for simulating the spatiotemporal distribution characteristics of dust aerosol content in China (Kang et al., 2016; Wang et al., 2021). It is reported that the result based on MERRA-2 are similar to those obtained from MODIS, OMPS, CALIPSO, and Himawari-8 data (Kang et al., 2016; Wang et al., 2021). Additionally, we further employ the datasets from the China National Meteorological Centre from 1980-2018, which include observations of floating dust, blowing dust, and dust storms, to validate the reliability of MERRA-2 reanalysis data. The frequency of dust activities recorded at these stations has been converted into a Dust Index (DI) (Wang et al., 2008; Equations 1), effectively representing the content of dust aerosols.

$$\mathrm{DI} = 9 \times \mathrm{DS} + 3 \times \mathrm{BD} + 1 \times \mathrm{FD} \quad (1)$$

Where DS, BD, and FD represent the frequency of dust storms, blowing dust, and floating dust, respectively. Additionally, DI denotes the content of dust aerosols at each station. We found that the variations of the DI and MERRA-2 dust aerosols content during the four seasons all show similar spatial characteristics (Figure 1). Especially for the dust source in northwest China and the spring dust aerosols over North China, the spatial distribution characteristics are relatively consistent. The above results indicate that the MERRA-2 aerosol reanalysis data can capture the spatiotemporal characteristics of dust aerosol content in China, which is applicable for us to understand the variations in dust aerosol content in China.

Additionally, the SST dataset was derived from the Hadley Centre of the UK Met Office on a 1°×1° grid (Rayner et al., 2003). The atmospheric reanalysis datasets employed herein were provided from the Fifth Generation Reanalysis Version 5 (ERA5) of the European Centre for Medium-Range Weather Forecasts (ECMWF) with a resolution of 0.25°×0.25° on 37 vertical levels (Hersbach et al., 2020), including wind, geopotential height, and sea-level pressure, specific humidity, precipitation, and vorticity field. Considering the available period of all datasets, the common available period of 1979–2022 was selected. The winter is defined as December-February (December-January-February, DJF), with the winter 1979 corresponding to the average of December in 1979, January and February in 1980. To focus the investigation into the interannual variability, the linear trends of all variables were removed.

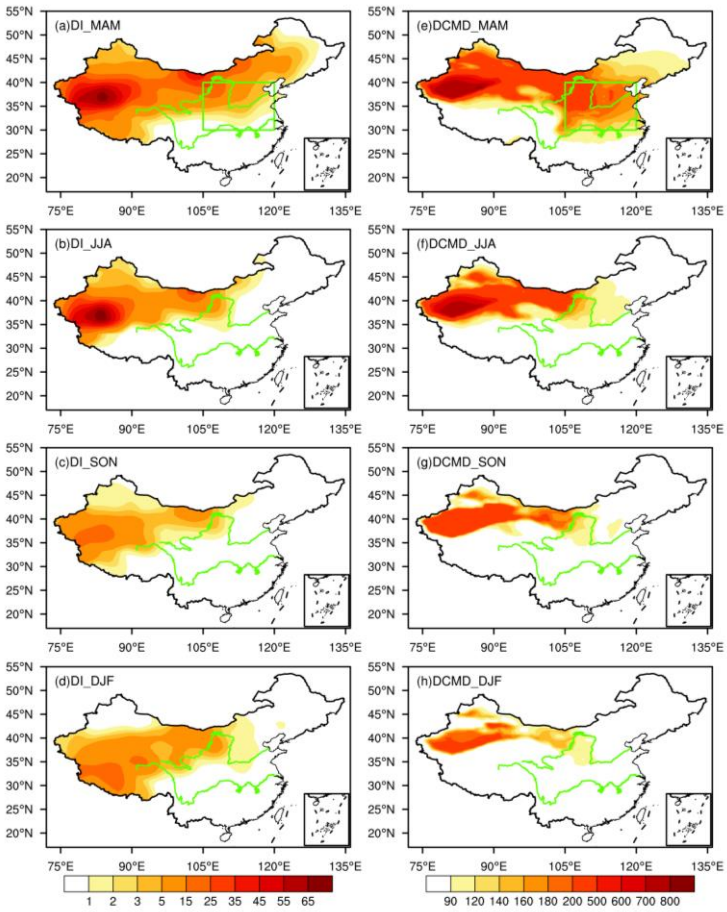

Figure 1. (a-d) Spatial distribution of seasonal mean DI based on station data, (e-h) as in (a-d), but for dust column mass density based on MERRA-2 (units: $mg \cdot m^{-2}$). The green box in (a) and (e) represents North China. The green lines represent the Yellow River (northern one) and the Yangtze River (southern one), respectively.

2.2 Methods

The NAO index (NAOI) used is following Li and Wang (2003), quantified by the difference in the normalized monthly SLP regionally zonal averaged over the North Atlantic within 80°W-30°E between 35°N and 65°N. This definition effectively captures the large-scale circulation characteristics associated with NAO, essentially measuring the intensity of zonal winds spanning the entire North Atlantic. We also employed the NAOI produce by Hurrell (1995) and Jones (1997), which have been used in many studies (e.g., Wang et al., 2022; Najibi et al., 2023; Parry et al., 2023). A good agreement with correlation coefficients of 0.96 and 0.94 between these two indices and the NAOI defined by Li and Wang (2003). Furthermore, ENSO is characterized by Niño3.4 index with SST anomalies averaged over 5°S-5°N, 170°W-120°W (Trenberth, 1997).

In this study, we utilized the standardized indices of seasonal averages during the previous winter (the winter from 1979 to 2021), with values exceeding 0.5 standard deviations identified as

anomalous years, as shown in Table 1. The winter NAO and ENSO indices are during 1979-2021, and the spring dust are during 1980-2022, to highlight the preceding impacts of previous winter on the following spring. The correlation analysis is used to explore the relationship between NAO/ENSO and dust content over North China, and the composite analysis is employed to investigate the synergistic effects of these climatic variabilities on the dust activities over North China. The statistical significance of the correlation, regression and composite values was evaluated by a two-sided Student's *t*-test.

The memory effect of SST can be elucidated by the SST persistence component (SST_p), as delineated in equation (2) (Pan, 2005).

$$SST_p = SST(t) * \frac{Cov[SST(t), SST(t+1)]}{Var[SST(t)]} \tag{2}$$

SST_p represents the memory effect of the previous SST (previous winter) on the following SST (spring), where $SST(t)$ and $SST(t+1)$ denote the previous winter SST and spring SST, respectively. $Cov[SST(t), SST(t+1)]$ denotes the covariance between the previous winter SST and spring SST, while $Var[SST(t)]$ signifies the variance of the previous winter SST. Consequently, the $Cov[SST(t), SST(t+1)]/Var[SST(t)]$ represents the connection between the SST variations in previous winter and spring. A greater value of SST_p indicates the variation of $SST(t+1)$ is more closely attached with the variation of $SST(t)$.

The T-N wave activity flux (WAF), formulated by Takaya and Nakamura (2001), represents a three-dimensional wave action flux that describes the energy dispersion characteristics of stationary Rossby waves, thereby reflecting the direction of Rossby wave energy dispersion. The WAF is suitable for application in mid-high latitude regions where the background circulation deviates from uniform zonality, as obviates the need for the assumption that the basic flow field must be a zonally averaged basic flow and can accommodate zonally non-uniform wind fields. The convergence and divergence characteristics of WAF reveal the source and dissipation areas of wave energy, with the transmission direction being interpretable as the direction of energy transport. The three-dimensional formulation of WAF is as follows:

$$W = \frac{pcos\varphi}{2|\boldsymbol{U}|} \cdot \begin{pmatrix} \frac{U}{a^2 cos^2\varphi}\left[\left(\frac{\partial\psi'}{\partial\lambda}\right)^2 - \psi'\frac{\partial^2\psi'}{\partial\lambda^2}\right] + \frac{V}{a^2 cos\varphi}\left[\frac{\partial\psi'}{\partial\lambda}\frac{\partial\psi'}{\partial\varphi} - \psi'\frac{\partial^2\psi'}{\partial\lambda\partial\varphi}\right] \\ \frac{U}{a^2 cos\varphi}\left[\frac{\partial\psi'}{\partial\lambda}\frac{\partial\psi'}{\partial\varphi} - \psi'\frac{\partial^2\psi'}{\partial\lambda\partial\varphi}\right] + \frac{V}{a^2}\left[\left(\frac{\partial\psi'}{\partial\varphi}\right)^2 - \psi'\frac{\partial^2\psi'}{\partial\varphi^2}\right] \\ \frac{f_0^2}{N^2}\left\{\frac{U}{acos\varphi}\left[\frac{\partial\psi'}{\partial\lambda}\frac{\partial\psi'}{\partial z} - \psi'\frac{\partial^2\psi'}{\partial\lambda\partial z}\right] + \frac{V}{a}\left[\frac{\partial\psi'}{\partial\varphi}\frac{\partial\psi'}{\partial z} - \psi'\frac{\partial^2\psi'}{\partial\varphi\partial z}\right]\right\} \end{pmatrix} \tag{3}$$

In the expression, p, φ, λ, f_0, and a represent the geopotential height, latitude, longitude,

coriolis parameter, and Earth's radius, respectively. $\psi' = \Phi'/f$ (where Φ represents the geopotential) denotes the disturbance of the quasi-geostrophic stream function relative to the climatology. The basic flow field $\boldsymbol{U} = (U, V)$ denotes the climatic field, where U and V indicate the zonal and meridional velocities, respectively.

3. Results

3.1 Impacts of NAO and ENSO on the spring dust in North China

The standard deviation of the NAO peaks during December, January, and February. By analyzing the three-month running average standard deviation, it is seen the maximum occurs during winter. This indicates that winter NAO exhibits stronger variability compared to other seasons (Figure 2a). Similarly, ENSO shows larger variation during winter (Figure 2b). Previous studies have found that preceding NAO and ENSO play important roles in impacting the following climate over North China, particularly the cross-seasonal impacts (e.g., Zheng et al., 2016; Feng et al., 2019; Sun et al., 2021). We have examined the roles of previous autumn, winter and simultaneous spring NAO and ENSO on the spring dust aerosols over North China. It is found that the most significant influences of NAO and ENSO on the spring dust aerosols occurs when the NAO and ENSO leading one season (Figures 2c-h). Therefore, the roles of previous winter NAO and ENSO on the spring dust aerosols over North China are discussed.

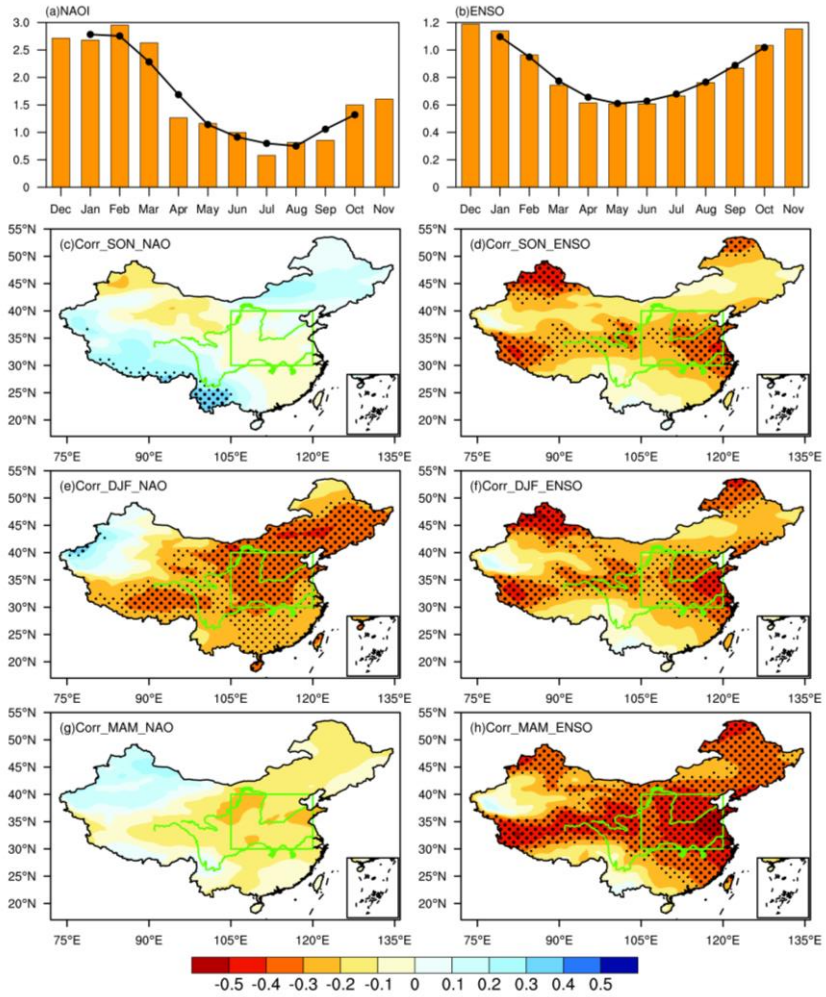

Figure 2. The monthly standard deviation of (a) NAOI and (b) Niño3.4 index, respectively. Black line represents three-month running average of standard deviation. (c) Spatial distribution of correlation coefficients between the previous autumn NAOI and spring dust content . (d) As in (c), but with Niño3.4 index. (e-f) and (g-h), as in (c-d), but for the correlations with previous winter and simultaneous spring NAOI and Niño3.4 index, respectively. The green box represents North China. Thick and fine stippled areas are statistically significant at the 0.05 and 0.1 level, respectively. The green lines in (c-h) represent the Yellow River (northern one) and the Yangtze River (southern one), respectively.

Previous studies have highlighted the significant impacts of NAO (e.g., Wu et al., 2009; Zheng et al., 2016a; Wang et al., 2018) and ENSO (e.g., Zhao et al., 2016; Zhang et al., 2016; Feng et al., 2020) on the climate anomalies over China. To investigate their effects on the spring dust, the correlations between the previous winter NAO/ENSO and following spring dust content are examined (Figure 3). Significant negative correlations are observed over North China between NAOI and dust content. Similar relationship is seen in the ENSO case. This result indicates that lower (higher) dust content is expected when the NAO and ENSO are in the positive (negative) phases (Figures 3a-b). Meanwhile, the NAOI/Niño3.4 index is significantly correlated with the areal

averaged spring dust content over North China (SDI), with correlation coefficient of -0.36/-0.35. Considering the significant interaction between NAO and ENSO (López-Parages et al., 2015; Zhang et al., 2015), to detect their independent effects on the dust content, the partial correlation between NAO (ENSO) and dust content after removing the influence of the ENSO (NAO) are provided. The results indicate that the significant correlation regions between dust content and either the NAO or ENSO show little change after removing the influence of the other. These findings suggest a stable and significant connection between the previous winter NAO and ENSO and the dust content in North China (Figures 3c-d).

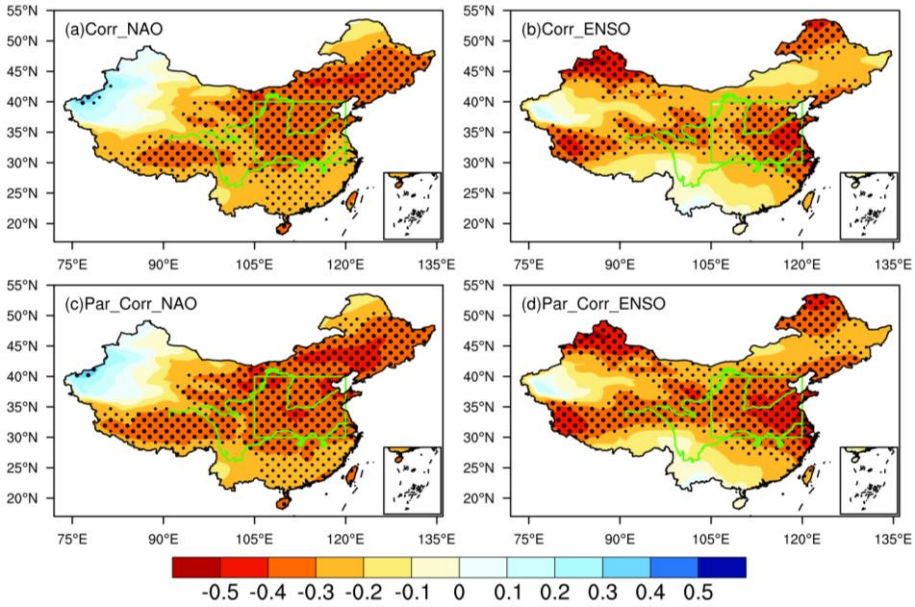

Figure 3. (a) Spatial distribution of correlation coefficients between the previous winter NAOI and spring dust content. (b) As in (a), but with Niño3.4 index. (c) As in (a), but for the partial correlation after removing the effect of ENSO. (d) As in (c), but after removing the effect of NAO. The green box represents North China. Thick and fine stippled areas are statistically significant at the 0.05 and 0.1 level, respectively. The green lines represent the Yellow River (northern one) and the Yangtze River (southern one), respectively.

Previous studies have indicated that the development rate, intensity variations, and the spatial structure of NAO exhibit distinct asymmetric characteristics between different phases (Feldstein, 2003; Jia et al., 2007). Furthermore, the influence of NAO on the EAWM is more pronounced during its negative phase (Sung et al., 2010). Similarly, both observational facts and model experiments suggest that El Niño and La Niña, as the positive and negative phases of ENSO, are not simply mirror images of each other. The SST anomalies in the tropical Pacific associated with ENSO exhibit significant asymmetry in terms of meridional range (Zhang et al., 2009), amplitude (Su et al., 2010), zonal propagation (McPhaden and Zhang, 2009), as well as climate impact (Feng and Li, 2011; Feng et al., 2020) under El Niño and La Niña conditions. Consequently, we further analyzed the

connection between NAO/ENSO and spring dust but in different phases. The results indicate that the relationship between NAO/ENSO and dust in North China also exhibits significant asymmetry, i.e., with weaker (stronger) correlations during positive (negative) phases of NAO and ENSO (Figure 4), where significant correlations only appear in the negative phases of NAO and ENSO. Based on the scatter distribution of SDI under different phases of NAO and ENSO, it is noted that the correlation coefficients between NAOI and SDI during the positive and negative phases of NAO are -0.46 and -0.05, respectively, indicating that the significant influence of NAO on the dust in North China mainly occurs during its negative phase (Figure 5a). Similarly, the correlation distribution between the ENSO and SDI also shows that the influence of ENSO is more pronounced during its negative phase (Figure 5b). These results indicate that the impacts of previous winter NAO and ENSO on the spring dust content in North China exhibit asymmetrical characteristics, significant effects mainly manifested during their negative phases.

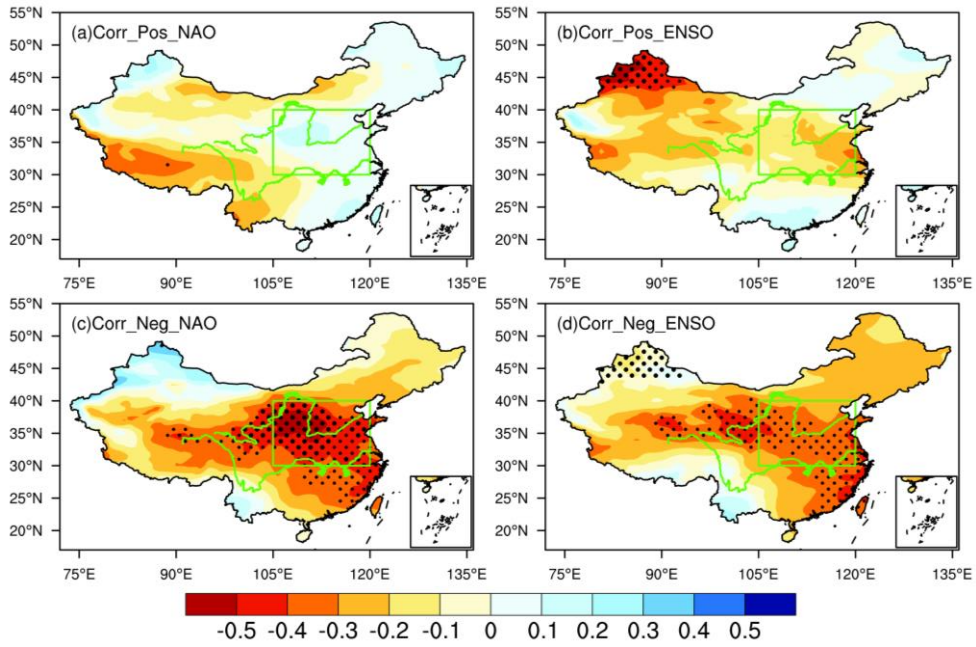

Figure 4. Spatial distribution of correlation coefficients between (a) positive and (c) negative NAOI values and dust content. (b) and (d) as in (a) and (b), respectively, but for the Niño3.4 index. The green box represents North China. Thick and fine stippled areas are statistically significant at the 0.05 and 0.1 level, respectively. The green lines represent the Yellow River (northern one) and the Yangtze River (southern one), respectively.

The synergistic effects of climate variabilities from mid-high latitudes and tropics are pivotal mechanisms affecting the weather and climate in East Asia (Feng et al., 2019; Li et al., 2019). Correspondingly, we will examine whether the negative phases of previous winter NAO and ENSO exert synergistic effects on the following spring dust content in North China. As shown in Figure 5c, when the NAO is in its negative phase (Table 1; white bar in Figure 5c labeled NAO), the value

of anomalous dust content over North China is +16.21 mg·m^{-2}, whereas it is +8.32 mg·m^{-2} for the case that negative NAO occurred alone (red bar in Figure 5c). Similarly, the value of dust content anomalies over North China in the negative ENSO phase is greater than that when negative ENSO occurred alone (+19.40 mg·m^{-2} vs. +14.88 mg·m^{-2}). When the NAO and ENSO both are in negative phases (Table 1), the value of dust content anomalies (+25.23 mg·m^{-2}) is much greater than the situation when one of them is in the negative phase (green bar in Figure 5c). That is the negative phases of previous winter NAO and ENSO demonstrate synergistic effects on the spring dust activities in North China. Therefore, three categories, i.e., the NAO (ENSO) is in its negative phase, and both the NAO and ENSO are in the negative phases simultaneously (Table 1) are discussed in the context to elucidate the relevant processes of the synergistic effects of NAO and ENSO on the dust content over North China.

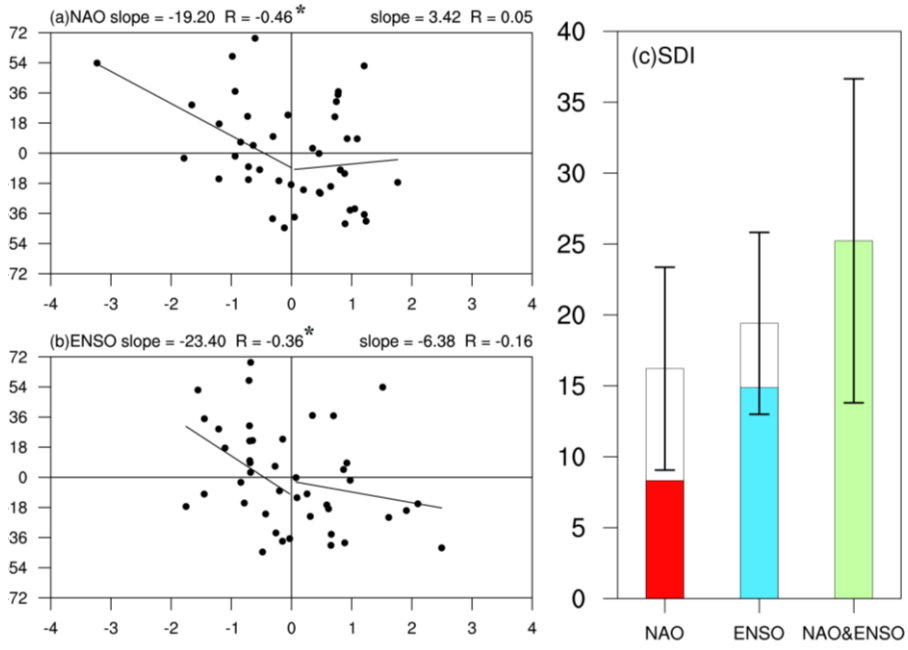

Figure 5. Scatterplots of the spring dust content in North China against previous winter (a) NAOI and (b) Niño3.4 index. Also shown are lines of best fit for positive and negative NAO/Niño3.4 index values and correlation coefficients (R), slope (slope), * indicates significant at the 0.1 level. (c) Spring dust content over North China during the negative NAO, negative ENSO phases, and concurrent negative phases of NAO and ENSO (unit: mg·m^{-2}). White bars represent negative phases of the NAO and ENSO, red and blue bars indicate solo negative NAO and ENSO years, and green bar is the negative NAO and ENSO co-occurring years.

Table 1. The events of NAO and ENSO classified by three categories

Scenarios	Years	Numbers
NAO$^-$	1980,1982,1985,1986,1987,1996,1998,2001, 2003,2004,2006,2010,2011,2013,2021	15
ENSO$^-$	1984,1985,1986,1989,1996,1999,2000,2001,	16

	2006,2008,2009,2011,2012,2018,2021,2022	
NAO^- &$ENSO^-$	1985,1986,1996,2001,2006,2011,2021	7

3.2 Impacts of NAO and ENSO on the environmental variables

To examine the anomalous characteristics associated with NAO and ENSO, the circulation anomalies in their negative phases, as well as in their co-occurring negative phases (Table 1) are analyzed. In the upper troposphere (200 hPa), the zonal wind is strengthened over the northwest of China and Mongolia during the negative NAO phase (Figure 6a), with evident positive anomalies centered on Mongolia. In the case of negative ENSO phase, the upper-level zonal wind also shows an intensification over the northwest region of China and Mongolia (Figure 6d). The intensification of upper-level zonal wind boosts the upper-level momentum, which is subsequently transferred downward to the mid-lower troposphere through vertical circulation (Wu et al., 2016; Li et al., 2023), causing windy weather in the surface dust source regions, facilitating dust lifting and transport activities, thereby promoting the occurrence of dust activities in the downstream North China. When both the NAO and ENSO are in their negative phases, the main positive anomaly center appears over North China, which is stronger than the situation in either the NAO or ENSO. This result implies the synergistic effects of NAO and ENSO on the upper-level zonal wind, facilitating an enhanced transport of dust from its source regions to North China, consequently triggering the onset of dust activities conditions in North China (Figure 6g).

Subsequent analysis delved into the anomalous distribution of the circulation field in the mid and lower troposphere. In the negative NAO situation, a pronounced “trough-ridge” anomaly pattern emerges in the mid-latitude region, characterized by a trough in Siberia and a ridge in the Middle East (Figure 6b). This atmospheric configuration fosters a dominant meridional circulation in the mid-high latitude region, thereby facilitating the enhanced transport of cold air from the north. Such a southward incursion of cold air serves to strengthen the surface wind speeds, and to promote the uplift and transport of dust from the source regions. In the negative ENSO situation, although the mid-latitude region exhibits a similar trough-ridge pattern, more pronounced circulation anomalies are observed over the WNP. At this time, the region is predominantly under the influence of northeasterly winds on its western flank, manifesting cyclonic circulation anomalies (Figure 6e), consistent with previous research results (Ke et al., 2023). This abnormal circulation will hinder the northward transport of warm and moist air from the South China Sea and the Bay of Bengal, diminishing the likelihood of interactions with cold air from the north, thus reducing the possibility of forming of stationary fronts and precipitation. The decrease in precipitation weakens the wet

deposition effect (Zheng et al., 2016b; Huang et al., 2021), favoring the occurrence of dust activities in the region. When both the NAO and ENSO are simultaneously occurred, the meridional circulation in the mid-latitude region is enhanced (Figure 6h). Furthermore, the southward shift of the trough-ridge pattern leads to a more significant increase in wind speed in the upstream dust source regions of North China, providing a more substantial source of dust for North China. Meanwhile, the presence of a cyclonic circulation anomalies over the WNP reduces the transport of warm and moist air from the south, which is unfavorable for precipitation, thereby lowering the wet deposition effect on dust and further favoring the onset and intensification of dust activities in North China.

As for the SLP, significant positive SLP anomalies appear in Eastern Europe and Russia during negative NAO situation, indicative of an intensified Siberian High (SH), which extends southward to the dust source regions upstream of North China (Figure 6c). The intensification of the SH is typically accompanied by strong northerlies and dry conditions, favoring the transport of dust, thereby supplying abundant material sources for dust activities in North China. In the negative ENSO case, although the high-latitude region exhibits a weaker SH signal, similar to the ENSO influence on the circulation pattern in the middle and lower troposphere, more significant circulation anomalies occur over the WNP. This cyclonic circulation anomalies inhibit the northward transport of warm and moist air from the south, leading to unfavorable precipitation conditions in North China (Figure 6f). When both the NAO and ENSO are in their negative phases, the intensify and extent of the SH are more pronounced compared to that when the NAO sole is in negative phase. Additionally, cyclonic circulation anomalies persist over the WNP, which are conducive to the occurrence of dust events in North China (Figure 6i).

The results suggest that when both the NAO and ENSO are in their negative phases, synergistic effects emerge, rendering the atmospheric circulation in the troposphere more conducive to the occurrence of dust events in North China. The synergistic effects may be due to the superposition and interaction of various atmospheric levels and regional characteristics modulated by the NAO and ENSO, thereby forming more favorable circulation conditions for dust activities in North China.

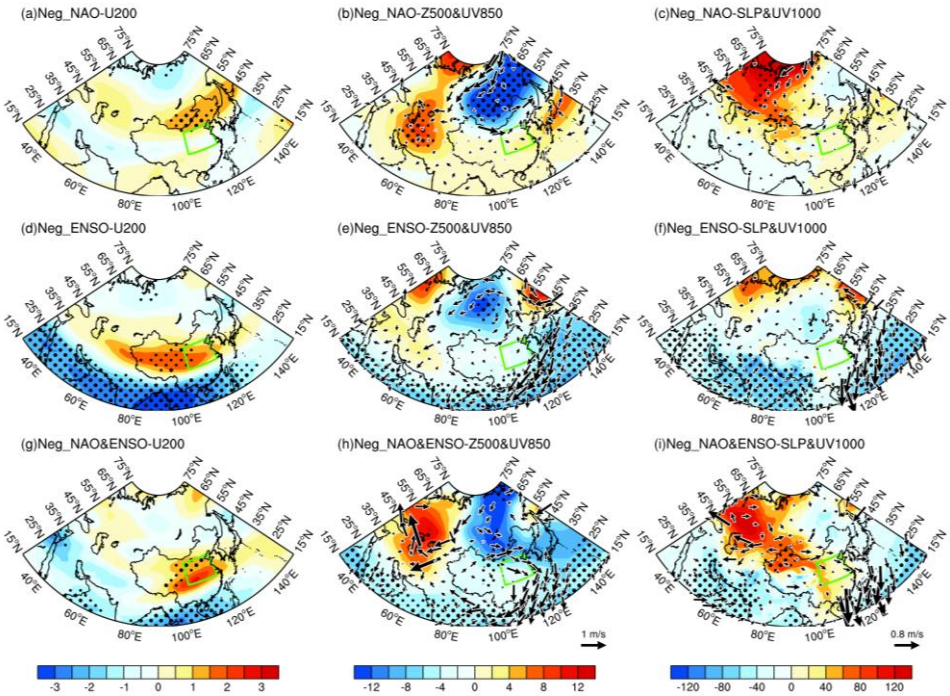

Figure 6. Upper, the composite anomalies of (a) 200 hPa zonal wind (shading, unit: $m \cdot s^{-1}$), (b) 500 hPa geopotential height (shading, unit: gpm) and 850 hPa wind field (arrows, unit: $m \cdot s^{-1}$), (c) sea-level pressure (shading, unit: Pa) and 1000 hPa wind field (arrows, unit: $m \cdot s^{-1}$) during the negative NAO phases. Middle-Lower, as in the upper, but during the negative ENSO phases and co-occurred negative phases of NAO and ENSO, respectively. The green box represents North China. Only wind anomalies statistically significant at the 0.1 level are shown. Thick and fine stippled areas are statistically significant at the 0.05 and 0.1 level, respectively.

Dust activities are multifaceted phenomena related to large-scale circulation patterns, and significantly influenced by local surface conditions and meteorological processes. Surface properties and local meteorological factors play a role in the initiation, development, and dissipation of dust activities (e.g., Liu et al., 2004; Yao et al., 2021; Huang et al., 2021). In particular, humidity and precipitation play decisive roles in determining the frequency and intensity of dust activities (Prospero et al., 1987; Kim and Choi, 2015). Low humidity leads to drier soil conditions in the dust source regions, reducing the cohesion between soil particles and facilitating dust lifting and transport activities (Csavina et al., 2014), and vice versa. Similarly, the amount of precipitation directly affects the wet deposition process of dust. Less precipitation weakens the wet deposition, associated with relatively higher dust content (Zheng et al., 2016b). Therefore, we further analyzed their potential impacts on the humidity and precipitation. When the NAO is in its negative phase, humidity in the spring dust source regions and North China is generally reduced, particularly in areas near the dust source regions, indicating that these areas are conducive to dust transport and prone to causing dust activities in North China (Figure 7a). As for the precipitation, there is more spring precipitation in the northwest region of China, while precipitation in the Mongolia and the

North China is relatively less (Figure 7b). In the negative ENSO phase, the variation in humidity is similar to that during the negative NAO phase, but with a greater amplitude (Figure 7c), indicating that ENSO has a stronger impact on the humidity conditions in North China. Moreover, the precipitation shows a significant decrease over Mongolia and North China, which is highly conducive to dust activities (Figure 7d). When both the NAO and ENSO are in the negative phases, the humidity anomalies in the dust source regions and North China are more intense than the individual factor (Figure 7e). The variation in precipitation is similar to those in humidity, the reduction in precipitation in the dust source regions and North China exceeds the sole role (Figure 7f). The aforementioned analysis indicates that the NAO and ENSO can modulate humidity and precipitation, ultimately affecting dust activities. During the negative NAO case, the diminished atmospheric pressure gradient in the mid-high latitude regions of North Atlantic leads to the intensification and southward shift of the SH (Zhou et al., 2023), accompanied with strong wind, making the environment drier and conducive to dust lifting and transport in the dust source regions. In the negative ENSO case, the upper atmosphere over the WNP is dominated by significant negative anomalies in geopotential height and northeasterly winds (Zhang et al., 2015), reducing moist transport. When the NAO and ENSO both are in negative phases, their regulation of atmospheric circulation produces synergistic effects, further influencing the variations of humidity and precipitation, thereby promoting the occurrence and development of dust activities in North China.

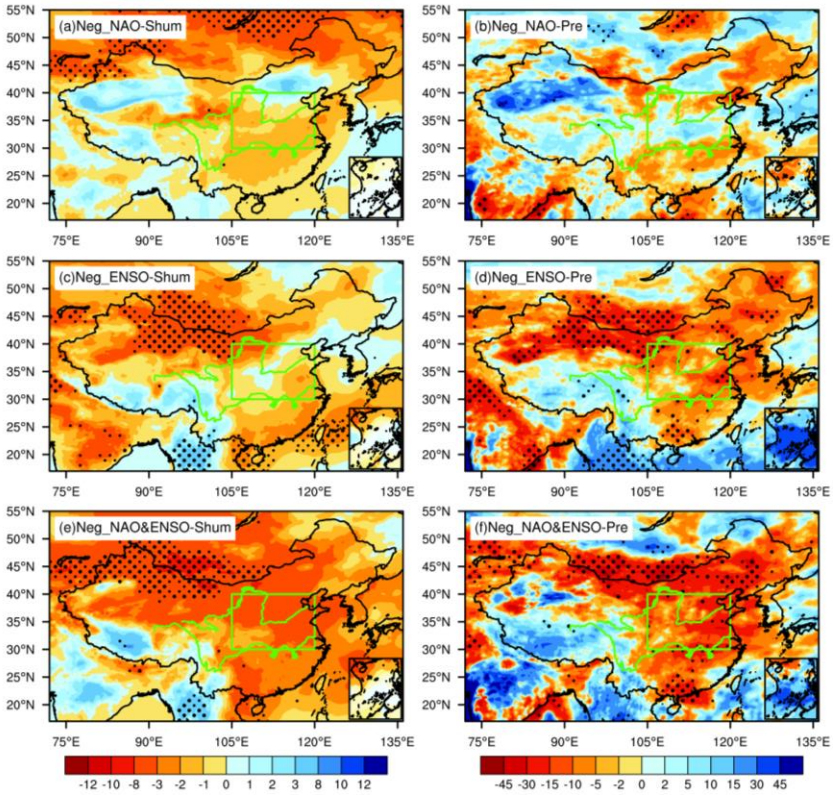

Figure 7. As in Figure 6, but for the composite percentage anomalies of (Left) special humidity and (Right) precipitation.

3.3 Physical Mechanisms of the NAO and ENSO on the dust activities

The above results demonstrate that the previous winter NAO and ENSO exert significant impacts on the spring dust activities in North China. Consequently, an examination of the underlying physical mechanisms is warranted. Given the relatively short memory of NAO as an atmospheric phenomenon, we will employ the concept of ocean-atmosphere coupling bridge to elucidate the involved processes. The previous ENSO signal can alter the atmospheric circulation over the WNP through the persistent impact of SST, thereby significantly affecting subsequent weather and climate in China (e.g., Wu et al., 2017; Kim and Kug, 2018; Jiang et al., 2019). The tripole configuration of SST is the leading mode of SST variation in the North Atlantic, and its variabilities are closely associated with the NAO (Wu et al., 2009), allowing the previous NAO signal to exert a long-term influence on the subsequent weather and climate in China (e.g., Chen et al., 2020; Wu and Chen, 2020; Song et al., 2022). The variation of SDI is linked with an anomalous tripole SST in the North Atlantic (Figure 8a), paralleling with the SST anomalies accompanied with the negative phase of NAO. Therefore, the North Atlantic tripole index (NATI) is defined to depict the characteristics of SST anomalies (Equations 4-7), as well as the relationships among the NAOI, NATI, and SDI are

explored. The correlation analysis between the high and low years of SDI and NATI reveals a pronounced difference, indicating an asymmetric correlation (Figures 8b-c). Specifically, the significant relationship between SDI and NATI only existed in the positive SDI years, implying that the occurrence of NATI would connect with more dust activities over North China.

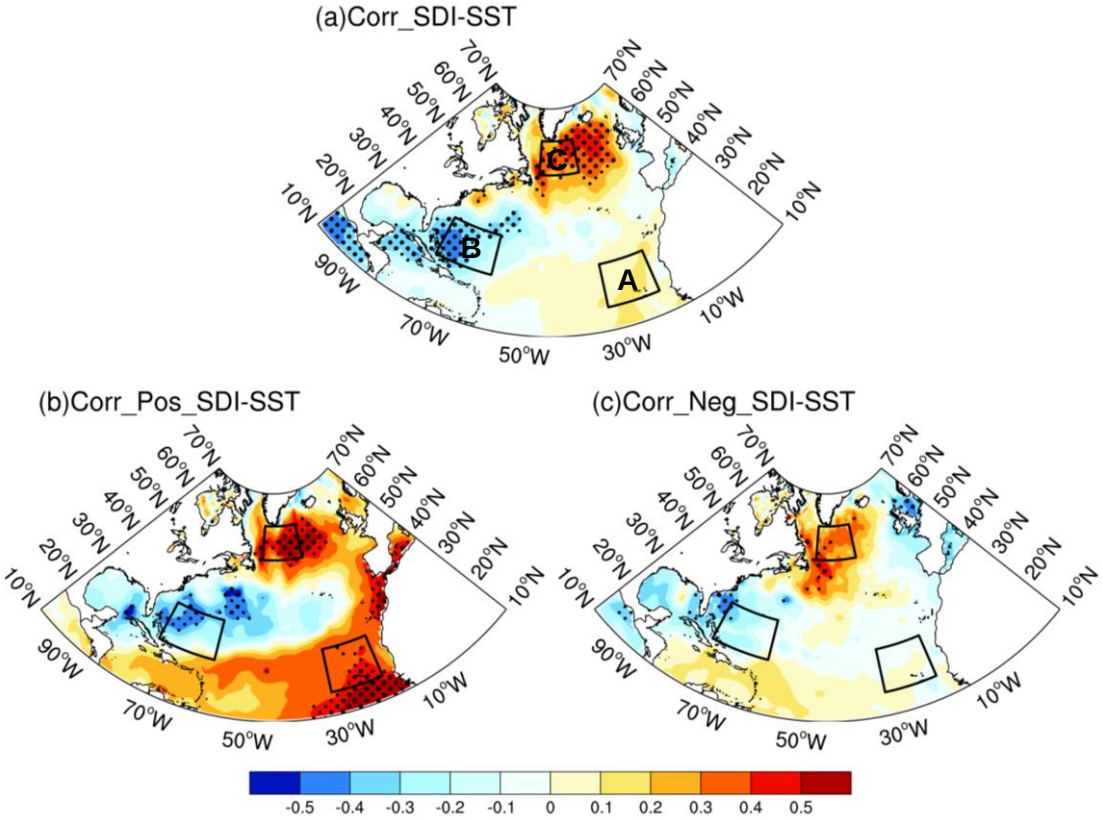

Figure 8. (a) Spatial distribution of the correlation coefficients between the spring SDI and simultaneous SST. (b)-(c) As in (a), but for the positive and negative phase of SDI. Thick and fine stippled areas are statistically significant at the 0.05 and 0.1 level, respectively. The black box represents NATI.

$$\mathrm{SST_A} = [15{-}25^{\circ}\mathrm{N}, 32{-}20^{\circ}\mathrm{W}] \quad (4)$$

$$\mathrm{SST_B} = [22{-}32^{\circ}\mathrm{N}, 75{-}60^{\circ}\mathrm{W}] \quad (5)$$

$$\mathrm{SST_C} = [50{-}60^{\circ}\mathrm{N}, 50{-}32^{\circ}\mathrm{W}] \quad (6)$$

$$\mathrm{NATI} = \mathrm{SST_B} - \frac{1}{2}(\mathrm{SST_A} + \mathrm{SST_C}) \quad (7)$$

Subsequent analyses delved into the association between the previous winter NAO and the North Atlantic SST. It is seen that the correlation coefficients between the negative (positive) NAOI and NATI are 0.41(-0.09) (figures not shown), indicating that the influence of previous winter NAO on the following spring NATI only manifest during its negative phase. This elucidates the reason why the significant impact of NAO on the dust activities in North China only existed during its negative phase. In the negative NAO phase, there is a notable correlation between the previous

winter NATI and the spring SST and SST_p (Figures 9b-c), indicating that the previous winter NATI can persist into spring, in which the self-persistence of SST playing a crucial role. Similar findings are observed during the negative phase of ENSO (Figures 9e-f) and when both the NAO and ENSO occur simultaneously (Figures 9h-i).

The correlation between the previous winter NAO and North Atlantic SST reveals that in the NAO negative situation (Figure 9a), the variation of NAO is linked with an anomalous tripole SST pattern in the North Atlantic. Meanwhile, similar findings are observed during negative ENSO situation (Figure 9d). This suggests that there may be positive feedback occurred between NAO and North Atlantic SST during negative ENSO phase. When both the NAO and ENSO are in the negative phases, the anomalous tripole SST pattern is more pronounced (Figure 9g). This further elucidates that ENSO exerts a promoting effect on strengthening the connection between the negative NAO and NATI, providing an explanation for the synergistic effects of the NAO and ENSO on the dust activities in North China. Additionally, the correlation coefficients between the NAOI and NATI under different scenarios can illustrate the synergistic influence of the NAO and ENSO on the persistence of SST anomalies (Table 2). Specifically, when the negative phase of NAO and ENSO occur together, the correlation coefficients between the NAOI and NATI are greater than those influenced by a single factor alone (Table 2). The impacts of previous winter NAO on the spring dust activities over North China are mainly include, 1) The previous winter NAO would stimulate the anomalous NAT SST pattern; 2) The NAT can last from previous winter to the following spring due to the thermal persistence of the SST; 3) The spring NAT plays significant modulation on the circulation pattern over North China through teleconnection wave trains, which ultimately affects the spring dust activities over North China. It is seen from Table 2 that although in the case of ENSO- phase and NAO- & ENSO- phase, the correlation coefficients of previous winter NATI and spring NATI are same. However, the correlations between the NAOI and NATI is higher during NAO- & ENSO- phase (0.66) than ENSO- phase (0.52), highlighting the significant role of NAO on the NAT in the case of NAO- & ENSO- phase. The above discussion illustrates the synergistic effect of NAO and ENSO on the dust activities over North China.

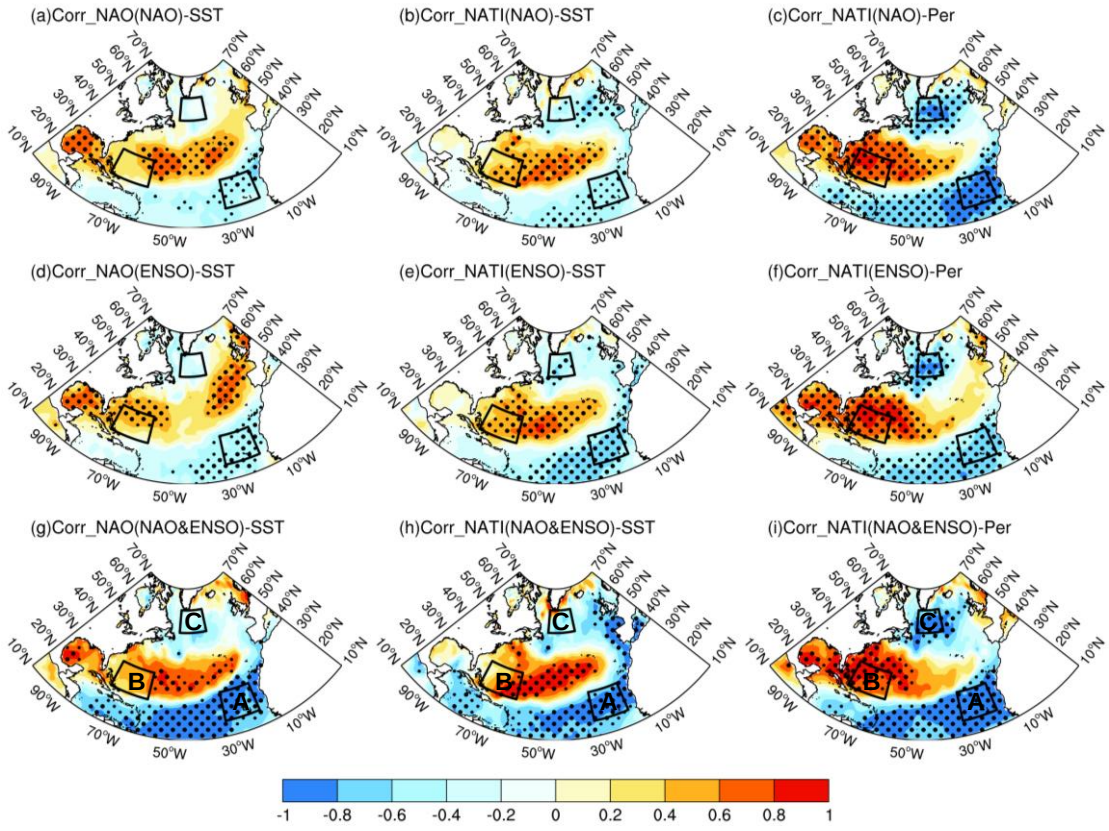

Figure 9. Upper, correlation distributions of the (a) winter NAOI with winter SST, (b) winter NATI with spring SST, and (c) winter NATI with SST_p during negative NAO phases. Middle-Lower, as in the upper, but during the negative ENSO phases and concurrent negative phases of NAO and ENSO, respectively. Thick and fine stippled areas are statistically significant at the 0.05 and 0.1 level, respectively. The black box represents NATI.

Table 2. Correlation coefficients between the NAOI and NATI in three different categories. * indicates significant at the 0.1 level.

Scenarios	DJF_NAO & DJF _NATI	DJF_NATI & MAM_NATI
NAO^- phase	0.41^*	0.51^*
$ENSO^-$ phase	0.52^*	0.69^*
NAO^- & $ENSO^-$ phase	0.66^*	0.69^*

The NAO preserves its anomalous signal within the tripole SST during the previous winter, and releases the anomalous signal in the following spring. Given the distance across the entire Eurasian continent between the North Atlantic and North China, the role of teleconnection wave trains is particularly important in influencing dust activities over North China. Figure 10a illustrates the geopotential height field at 200 hPa regressed onto the spring NATI during negative NAO case. This reveals a pronounced north-south reversed dipole pattern in the North Atlantic, i.e., negative over Azores and positive over Iceland, representing a typical negative NAO structure (e.g., Wallace and Gutzler, 1981; Hurrell, 1995; Li and Wang, 2003). Meanwhile, a positive-negative-positive

teleconnection wave train structure centered around eastern Europe, Middle East, and North China is observed, suggesting that the disturbance energy propagates downstream from the North Atlantic through waveguide effects, leading to anticyclonic circulation anomalies in North China. Similar teleconnection wave-train propagation characteristics are also observed in the 200 hPa meridional wind and vorticity fields (Figures 10b-c). During the negative ENSO case, modulated by the NATI, analogous teleconnection structures are also seen in the circulation field (Figures 10d-f). Notably, when the NAO and ENSO are both in their negative phases, the teleconnection structure reflected in the circulation field is more pronounced than when only one factor is dominated (Figures 10g-i), confirming the synergistic effects of both factors on the circulation processes affecting dust activities in North China.

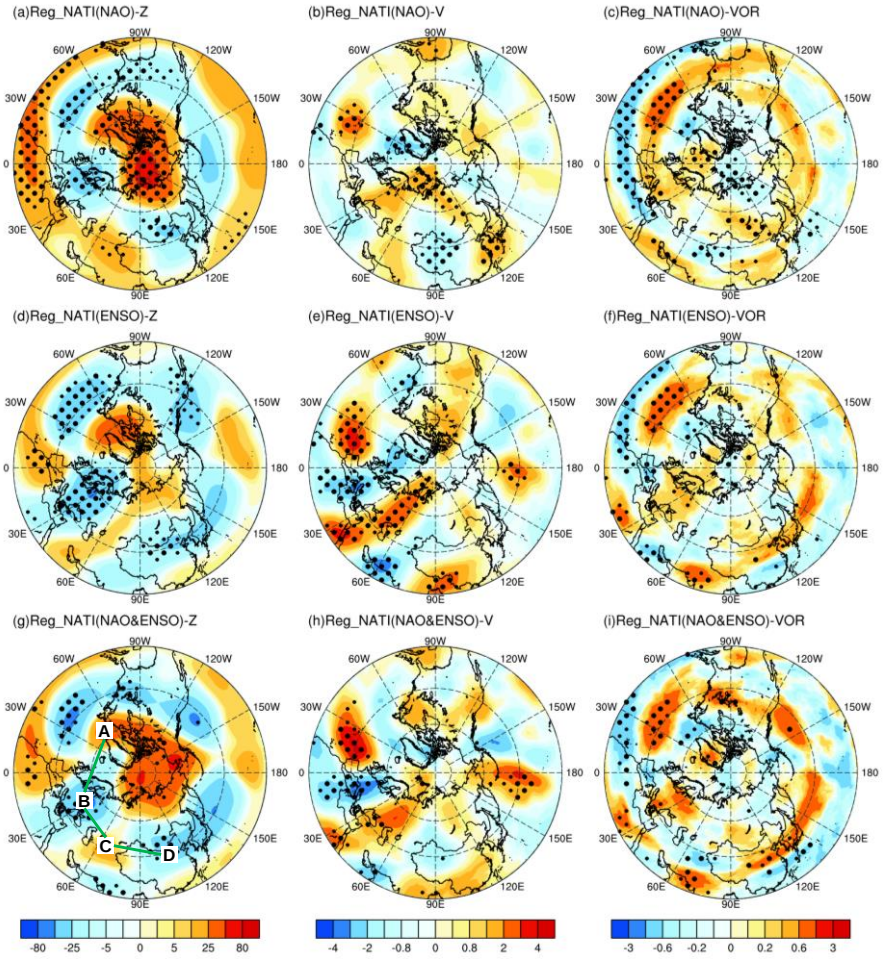

Figure 10. Upper, regression distribution of spring NATI against the spring (a) geopotential height (unit: gpm), (b) meridional wind (unit: $m \cdot s^{-1}$), and (c) vorticity (unit: $10^{-5} \cdot m \cdot s^{-1}$) at 200 hPa during the negative NAO phase. Middle-lower, as in the upper, but during the negative ENSO phases and concurrent negative phases of NAO and ENSO, respectively. Regression fields multiplied by -1. Thick and fine stippled areas are statistically significant at the 0.05 and 0.1 level, respectively.

To further examine the impact mechanisms of NAO and ENSO on the spring dust activities in

North China, based on the propagation characteristics of the teleconnection wave train shown in Figure 10, the distribution of cross-section of the geopotential height field is presented (Figure 11). When both the NAO and ENSO are in their negative phases, the NATI anomalies correspond to the teleconnection wave train extending from the upper to lower troposphere, which is specifically characterized by a positive-negative-positive tripole pattern. This wave train propagates from the North Atlantic, traversing eastern Europe and Middle East, and ultimately influencing circulation processes associated with the dust activities over North China. Furthermore, the analysis of cross-section at different levels of the troposphere reveals that under the negative NAO and ENSO situations, the teleconnection wave train excited by the NATI exhibits quasi-barotropic features, with this anomalous structure being primarily concentrated in the middle-upper troposphere. When the NAO and ENSO are simultaneously in their negative phases, the intensity and scope of the teleconnection wave train are significantly enhanced and expanded compared to the influence of a single factor (Figure 9c), demonstrating synergistic effects.

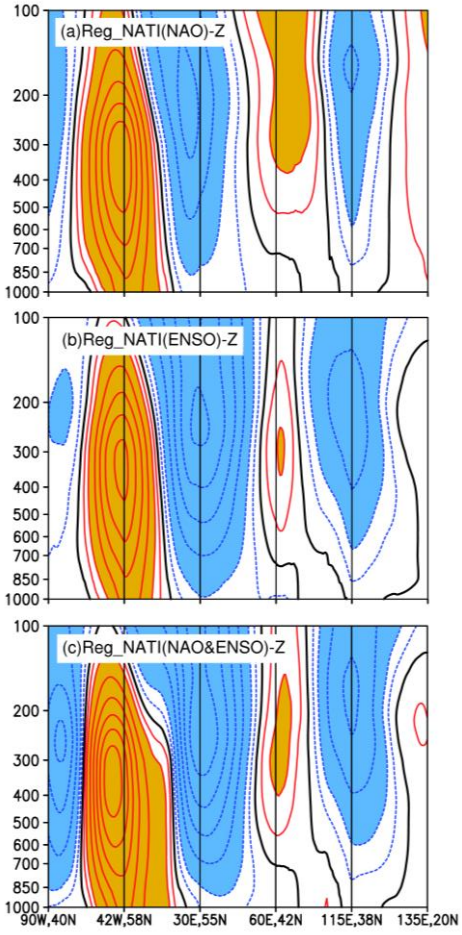

Figure 11. Vertical section of regression of spring NATI against the geopotential height along the solid line labeled A (42°W, 58°N), B (30°E, 55°N), C (60°E, 42°N), and D (115°E, 38°N) in Figure 10g for (a) negative NAO case in the previous winter. (b)-(c) as in (a), but during the negative ENSO

case and co-occurring negative phases of NAO and ENSO, respectively (unit: gpm). Regression fields have multiplied by -1. Shading indicates the absolute value is greater than 10 gpm.

To provide a more comprehensive analysis of the transport process of disturbance energy in the atmosphere, the horizontal distribution of the WAF associated with spring NATI variations is further examined. Under the scenario that either the NAO or ENSO is in their negative phases, WAF can be clearly observed to originate from the North Atlantic, traverse the Eurasian continent, and extend to the North China (Figures 12a-b). When both factors occur simultaneously, not only is the transport intensity of WAF enhanced, but its impact range on the dust activities in North China is also broadened (Figure 12c). Through the analysis of teleconnection wave trains and WAF, it is determined that the synergistic effects not only enhance the disturbance intensity in the atmosphere but also expand impacted extent, thereby promoting the occurrence and development of spring dust activities in North China. The enhancement and expansion of atmospheric disturbances may be related to large-scale circulation anomalies and local climate condition changes induced by the synergistic effects of the NAO and ENSO, which in turn affect the transport and deposition processes of dust.

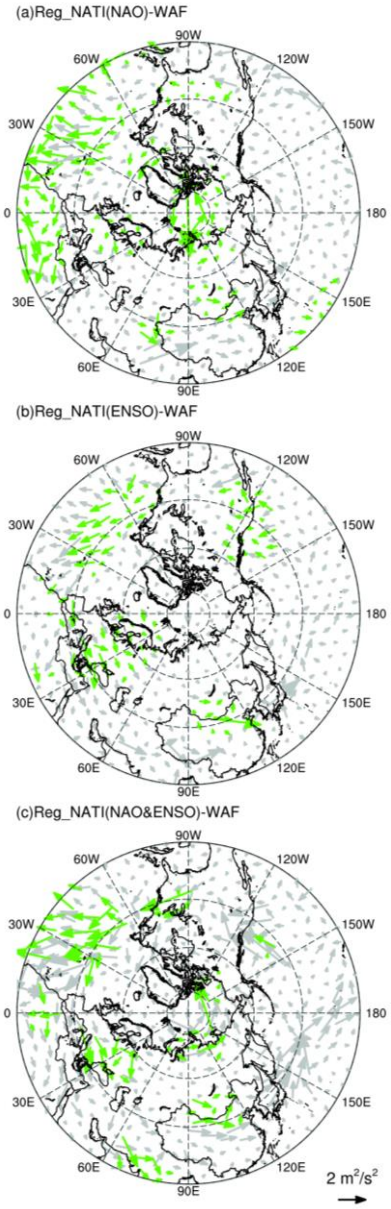

Figure 12. As in Figure 10, but for the regression distribution of spring NATI against the T-N wave activity flux (units: $m^2 \cdot s^{-2}$). Regression fields have multiplied by -1. Green arrows are statistically significant at the 0.1 level.

4. Conclusions and discussions

The NAO and ENSO exert significant impacts on climate variability in China (e.g., Zhang et al., 2016; Wang et al., 2018; Feng et al., 2020). Although North China is not the primary dust source, dust activities are notably active during spring in this region. This study highlights that the previous winter NAO and ENSO exert essential influences on the following spring dust activities in North China. Their impacts are asymmetric, manifesting only when both are in their negative phases. Furthermore, the results indicate that NAO and ENSO in the negative phase have synergistic effects

on the spring dust activities in North China, promoting dust activities and with greater impacts than their sole effect.

Under the regulatory influence of the negative phases of NAO and ENSO, the atmospheric circulation in the troposphere from the lower to upper layers, exhibits anomalies. These include variations in the upper-level zonal winds, mid-latitude trough-ridge systems, circulation over the WNP, and the SH at the SLP. These variations promote the occurrence and development of dust activities in North China. Simultaneously, accompanying anomalies in the atmospheric circulation pattern also affect local meteorological factors, including humidity and precipitation, which in turn impact the dust activities in North China. Notably, when both the NAO and ENSO are in their negative phases, synergistic effects occur, making the anomalies in atmospheric circulation from the lower to upper layers, as well as variations in humidity and precipitation, more conducive to the occurrence of dust events in North China. The impact of NAO on the underlying SST pattern is predominantly observed during its negative phase, elucidating why the NAO significantly influences dust activities in North China only during its negative phase. Furthermore, when both the NAO and ENSO simultaneously manifest in their negative phases, the teleconnection wave trains and WAF stimulated from the North Atlantic are more intense, thereby more effectively influencing dust activities in North China. This indicates the synergistic effects of the two variabilities on dust activities over North China.

In the process where the previous winter NAO and ENSO affect the following spring dust activities in North China, the persistence of anomalous NAT over North Atlantic plays an important role. The previous winter NAO stores its signal in the NAT (Wu et al., 2009). Due to the persistence of SST, the anomalous NAT can last from winter to spring (e.g., Wu et al., 2012; Zhang et al., 2021a; Li et al., 2023). In spring, NAT regulates the circulation pattern in North China through teleconnection wave trains, ultimately affecting the dust activities over North China. The signal of previous winter ENSO can persist into spring, due to the persistence of SST, and it affects the dust activities in North China through two pathways: i.e., directly influencing the dust activities in North China by affecting the circulation anomalies over the WNP, and playing a facilitating role in the process where the NAO excites NAT, thereby affecting the dust activities in North China. This provides a plausible explanation for why the previous winter NAO and ENSO exert synergistic effects on the following spring dust activities in North China.

This study investigated the impacts of NAO and ENSO on the dust activities in North China and the involved physical processes, indicating that one season ahead signals provide as the useful

predictors for spring dust activities in North China. Future work will focus on developing a prediction model using the NAO and ENSO as predictors and validating its prediction effectiveness. Additionally, as previous studies have highlighted strong interdecadal variations in both the NAO and ENSO (e.g., Woollings et al., 2015; Wang et al., 2023; Feng et al., 2024), it is of interest to further detect whether the synergistic effects of NAO and ENSO on the dust activity over North China experience interdecadal variations. However, due to the availability of dataset, the potential impacts of the interdecadal variability of the NAO and ENSO on dust activities have not been discussed in this study. Simultaneously, as reported that the state-of-art models can reproduce the individual impact of NAO and ENSO on the dust activities in North China (Yang et al., 2022), whether their synergistic effects on the dust activities could be well simulated, requiring further researches. Additionally, previous studies have indicated that the uncertainty in ENSO variability is likely to increase under the background of global warming (Cai et al., 2021; Chen et al., 2024). Therefore, it is crucial to investigate the future changes in the NAO, as well as future change of its synergistic effects with the ENSO on the dust activities, to better understand the plausible trends of future dust activities in North China. The present study is focused to period 1979-2022, due to the longevity of the MERRA-2 dust aerosol. There are only 7 co-occurrence years of negative NAO and ENSO. The co-occurrence of negative NAO and ENSO takes up to 17% of the whole study period. To be noted is that the sample are not long enough, it is worthy to examine their joint impacts by employing longer datasets or models outputs, to further detect their synergistic effects as well as any possible variations in their modulations. This study did not discuss the potential impacts of interdecadal signals, such as the AMO, on dust activities in China. The interdecadal variations of dust activities over China as well as its connection to the interdecadal climatic variabilities will be discussed in future work.

Code and data availability. The MERRA-2 dust aerosol content dataset can be downloaded from https://disc.gsfc.nasa.gov/datasets?project=MERRA-2 (last access: 7 July 2024). The atmospheric reanalysis datasets, including wind, geopotential height, and sea-level pressure, specific humidity, precipitation, and vorticity field can be downloaded from https://cds.climate.copernicus.eu/#!/search?text=ERA5&type=dataset (last access: 7 July 2024). The oceanic reanalysis data can be downloaded from https://www.metoffice.gov.uk/hadobs/hadisst (last access: 7 July 2024). The NAO indices defined by Li and Wang can be downloaded from http://lijianping.cn/dct/page/65610 (last access: 7 July 2024). The NAO indices produce by Hurrell

and Jones can be downloaded from https://climatedataguide.ucar.edu/climate-data/hurrell-north-atlantic-oscillation-nao-index-pc-based (last access: 7 July 2024) and https://crudata.uea.ac.uk/cru/data/nao (last access: 7 July 2024), respectively. The ENSO indices can be downloaded from https://psl.noaa.gov/data/timeseries/monthly/NINO34 (last access: 7 July 2024). Our results can be made available upon request.

Author contributions. JF and FLX conceptualized and designed the research. FLX and JF synthesized and analyzed the data. FLX, SW, YL, and JF produced the figures. FLX and SW contributed to the dataset's retrieval. All the authors discussed the results and wrote the paper.

Competing interests. The authors declare that they have no conflict of interest.

Disclaimer. Publisher's note: Copernicus Publications remains neutral with regard to jurisdictional claims in published maps and institutional affiliations.

Acknowledgements. The authors would like to thank two anonymous reviewers and editor Marco Gaetani for their useful comments and suggestions that contributed to improving the manuscript. This work was jointly supported by the National Natural Science Foundation of China (42222501) and the BNU-FGS Global Environmental Change Program (No. 2023-GC-ZYTS-03).

References

Abid, M. A., Kucharski, F., Molteni, F., Kang, I.-S., Tompkins, A. M., and Almazroui, M.: Separating the Indian and Pacific Ocean Impacts on the Euro-Atlantic Response to ENSO and Its Transition from Early to Late Winter, J. Climate, 34, 1531–1548, https://doi.org/10.1175/JCLI-D-20-0075.1, 2021.

Achakulwisut, P., Shen, L., and Mickley, L. J.: What Controls Springtime Fine Dust Variability in the Western United States? Investigating the 2002–2015 Increase in Fine Dust in the U.S. Southwest, J. Geophys. Res.-Atmos., 122, https://doi.org/10.1002/2017JD027208, 2017.

Ayarzagüena, B., Ineson, S., Dunstone, N. J., Baldwin, M. P., and Scaife, A. A.: Intraseasonal Effects of El Niño–Southern Oscillation on North Atlantic Climate, J. Climate, 31, 8861–8873, https://doi.org/10.1175/JCLI-D-18-0097.1, 2018.

Cai, W. J., Santoso, A., Collins, M., Dewitte, B., Karamperidou, C., Kug, J.-S., Lengaigne, M., McPhaden, M. J., Stuecker, M. F., Taschetto, A. S., Timmermann, A., Wu, L. X., Yeh, S.-W., Wang, G. J., Ng, B., Jia, F., Yang, Y., Ying, J., Zheng, X. T., Bayr, T., Brown, J. R., Capotondi, A., Cobb, K. M., Gan, B. L., Geng, T., Ham, Y.-G., Jin, F. F., Jo, H.-S., Li, X. C., Lin, X. P., McGregor, S., Park, J.-H., Stein, K., Yang, K., Zhang, L., and Zhong, W. X.: Changing El Niño–Southern Oscillation in a warming climate, Nat. Rev.-Earth Environ., 2, 628–644, https://doi.org/10.1038/s43017-021-00199-z, 2021.

Chen, S. F., Wu, R. G., and Chen, W.: Strengthened Connection between Springtime North Atlantic Oscillation and North Atlantic Tripole SST Pattern since the Late 1980s, J. Climate, 35, 2007–2022, https://doi.org/10.1175/JCLI-D-19-0628.1, 2020.

Chen, S. F., Chen W., Xie, S. P., Yu, B., Wu, R. G., Wang, Z. B., Lan, X. Q., and Graf. H .: Strengthened impact of boreal winter North Pacific Oscillation on ENSO development in warming climate, npj Climate and Atmospheric Science, 7, 69, https://doi.org/10.1038/s41612-024-00615-3, 2024.

Chen, S.Y., Zhao, D., Huang, J. P., He, J. Q., Chen, Y., Chen, J. Y., Bi, H. R., Lou, G. T., Du, S. K., Zhang, Y., and Yang, F.: Mongolia Contributed More than 42% of the Dust Concentrations in Northern China in March and April 2023, Adv. Atmos. Sci., 40, 1549–1557, https://doi.org/10.1007/s00376-023-3062-1, 2023.

Csavina, J., Field, J., Félix, O., Corral-Avitia, A. Y., Sáez, A. E., and Betterton, E. A.: Effect of wind speed and relative humidity on atmospheric dust concentrations in semi-arid climates, Sci. Total Environ., 487, 82–90, https://doi.org/10.1016/j.scitotenv.2014.03.138, 2014.

Ding, R. Q., Nnamchi, H. C., Yu, J. Y., Li, T., Sun, C., Li, J. P., Tseng, Y., Li, X. C., Xie, F., Feng, J., Ji, K., and Li, X. M.: North Atlantic oscillation controls multidecadal changes in the North Tropical Atlantic−Pacific connection, Nat. Commun., 14, 862, https://doi.org/10.1038/s41467-023-36564-3, 2023.

Fan, K., Xie, Z. M., Wang, H. J., Xu, Z. Q., and Liu, J. P.: Frequency of spring dust weather in North China linked to sea ice variability in the Barents Sea, Clim. Dyn., 51, 4439–4450, https://doi.org/10.1007/s00382-016-3515-7, 2018.

Feldstein, S. B.: The dynamics of NAO teleconnection pattern growth and decay, Q. J. Roy. Meteor. Soc., 129, 901–924, https://doi.org/10.1256/qj.02.76, 2003.

Feng, J. and Li, J. P.: Influence of El Niño Modoki on spring rainfall over south China, J. Geophys. Res.-Atmos., 116, D13102, https://doi.org/10.1029/2010JD015160, 2011.

Feng, J., Li, J. P., Liao, H., and Zhu, J. L.: Simulated coordinated impacts of the previous autumn North Atlantic Oscillation (NAO) and winter El Niño on winter aerosol concentrations over eastern China, Atmos. Chem. Phys., 19, 10787–10800, https://doi.org/10.5194/acp-19-10787-2019, 2019.

Feng, J., Wang, S., and Li, J. P.: Strengthened ENSO amplitude contributed to regime shift in the Hadley circulation. Geophys. Res. Lett., 51, e2023GL106006. https://doi. org/10.1029/2023GL106006, 2024.

Feng, J., Zhu, J. L., Li, J. P., and Liao, H.: Aerosol concentrations variability over China: two distinct leading modes, Atmos. Chem. Phys., 20, 9883–9893, https://doi.org/10.5194/acp-20-9883-2020, 2020.

Gelaro, R., McCarty, W., Suárez, M. J., Todling, R., Molod, A., Takacs, L., Randles, C. A., Darmenov, A., Bosilovich, M. G., Reichle, R., Wargan, K., Coy, L., Cullather, R., Draper, C., Akella, S., Buchard, V., Conaty, A., Da Silva, A. M., Gu, W., Kim, G.-K., Koster, R., Lucchesi, R., Merkova, D., Nielsen, J. E., Partyka, G., Pawson, S., Putman, W., Rienecker, M., Schubert, S. D., Sienkiewicz, M., and Zhao, B.: The Modern-Era Retrospective Analysis for Research and Applications, Version 2 (MERRA-2), J. Climate, 30, 5419–5454, https://doi.org/10.1175/JCLI-D-16-0758.1, 2017.

Gong, S. L., Zhang, X. Y., Zhao, T. L., Zhang, X. B., Barrie, L. A., McKendry, I. G., and Zhao, C. S.: A Simulated Climatology of Asian Dust Aerosol and Its Trans-Pacific Transport. Part II: Interannual Variability and Climate Connections, J. Climate, 19, 104–122, https://doi.org/10.1175/JCLI3606.1, 2006.

Guo, Y., Li, J. P., and Li, Y.: A Time-Scale Decomposition Approach to Statistically Downscale Summer Rainfall over North China, J. Climate, 25, 572–591, https://doi.org/10.1175/JCLI-D-11-00014.1, 2012.

Hersbach, H., Bell, B., Berrisford, P., Hirahara, S., Horányi, A., Muñoz-Sabater, J., Nicolas, J., Peubey, C., Radu, R., Schepers, D., Simmons, A., Soci, C., Abdalla, S., Abellan, X., Balsamo, G., Bechtold, P., Biavati, G., Bidlot, J., Bonavita, M., De Chiara, G., Dahlgren, P., Dee, D., Diamantakis, M., Dragani, R., Flemming, J., Forbes, R., Fuentes, M., Geer, A., Haimberger, L., Healy, S., Hogan, R. J., Hólm, E., Janisková, M., Keeley, S., Laloyaux, P., Lopez, P., Lupu, C., Radnoti, G., De Rosnay, P., Rozum, I., Vamborg, F., Villaume, S., and Thépaut, J.: The ERA5 global reanalysis, Q. J. Roy. Meteor. Soc., 146, 1999–2049, https://doi.org/10.1002/qj.3803, 2020.

Hu, Z. Y., Ma, Y. Y., Jin, Q. J., Idrissa, N. F., Huang, J. P., and Dong, W. J.: Attribution of the March 2021 exceptional dust storm in North China, B. Am. Meteorol. Soc., 104, E749–E755, https://doi.org/10.1175/BAMS-D-22-0151.1, 2023.

Huang, J., Li, Y., Fu, C., Chen, F., Fu, Q., Dai, A., Shinoda, M., Ma, Z., Guo, W., Li, Z., Zhang, L., Liu, Y., Yu, H., He, Y., Xie, Y., Guan, X., Ji, M., Lin, L., Wang, S., Yan, H., and Wang, G.: Dryland climate change: Recent progress and challenges, Rev. Geophys., 55, 719–778, https://doi.org/10.1002/2016RG000550, 2017.

Huang, J. P., Liu, J. J., Chen, B., and Nasiri, S. L.: Detection of anthropogenic dust using CALIPSO lidar measurements, Atmos. Chem. Phys., 15, 11653–11665, https://doi.org/10.5194/acp-15-11653-2015, 2015.

Huang, Y. H., Liu, X. D., Yin, Z., and An, Z. S.: Global Impact of ENSO on Dust Activities with Emphasis on the Key Region from the Arabian Peninsula to Central Asia, J. Geophys. Res.-Atmos., 126, e2020JD034068, https://doi.org/10.1029/2020JD034068, 2021.

Hurrell, J. W.: Decadal Trends in the North Atlantic Oscillation: Regional Temperatures and Precipitation, Science, 269, 676–679, https://doi.org/10.1126/science.269.5224.676, 1995.

Ji, L. Q. and Fan, K.: Climate prediction of dust weather frequency over northern China based on sea-ice cover and vegetation variability, Clim. Dyn., 53, 687–705, https://doi.org/10.1007/s00382-018-04608-w, 2019.

Jia, X. J., Derome, J., and Lin, H.: Comparison of the Life Cycles of the NAO Using Different Definitions, J. Climate, 20, 5992–6011, https://doi.org/10.1175/2007JCLI1408.1, 2007.

Jiang, W. P., Huang, G., Huang, P., Wu, R. G., Hu, K. M., and Chen, W.: Northwest Pacific Anticyclonic Anomalies during Post–El Niño Summers Determined by the Pace of El Niño Decay, J. Climate, 32, 3487–3503, https://doi.org/10.1175/JCLI-D-18-0793.1, 2019.

Jiménez-Esteve, B. and Domeisen, D. I. V.: The Tropospheric Pathway of the ENSO–North Atlantic Teleconnection, J. Climate, 31, 4563–4584, https://doi.org/10.1175/JCLI-D-17-0716.1, 2018.

Jones, P. D., Jonsson, T., and Wheeler, D.: Extension to the North AtlanticOscillation using early instrumental pressure observations from Gibraltar and South-West Iceland. Int. J. Climatol., 17, 1433–1450, https://doi.org/10.1002/(SICI)1097-0088(19971115)17:13<1433::AID-JOC203>3.0.CO;2-P, 1997.

Kang, L. T., Huang, J. P., Chen, S. Y., and Wang, X.: Long-term trends of dust events over Tibetan Plateau during 1961-2010, Atmos. Environ., 125, 188-198, https://doi.org/10.1016/j.atmosenv.2015.10.085, 2016.

Ke, M. L., Wang, Z. Q., Pan, W. J., Luo, H. L., Yang, S., and Guo, R. Y.: Extremely Strong Western Pacific Subtropical High in May 2021 Following a La Niña Event: Role of the Persistent Convective Forcing over the Indian Ocean, Asia-pac. J. Atmos. Sci., 59, 47–58, https://doi.org/10.1007/s13143-022-00300-6, 2023.

Kim, H. and Choi, M.: Impact of soil moisture on dust outbreaks in East Asia: Using satellite and assimilation data, Geophys. Res. Lett., 42, 2789–2796, https://doi.org/10.1002/2015GL063325, 2015.

Kim, S. and Kug, J.: What Controls ENSO Teleconnection to East Asia? Role of Western North Pacific Precipitation in ENSO Teleconnection to East Asia, J. Geophys. Res.-Atmos., 123, https://doi.org/10.1029/2018JD028935, 2018.

Kok, J. F., Storelvmo, T., Karydis, V. A., Adebiyi, A. A., Mahowald, N. M., Evan, A. T., He, C. L., and Leung, D. M.: Mineral dust aerosol impacts on global climate and climate change, Nat. Rev.-Earth Environ., 4, 71–86, https://doi.org/10.1038/s43017-022-00379-5, 2023.

Li, J. P., and Wang, J. X. L.: A new North Atlantic Oscillation index and its variability, Adv. Atmos. Sci., 20, 661–676, https://doi.org/10.1007/BF02915394, 2003.

Li, J. P., Zheng, F., Sun, C., Feng, J., and Wang, J.: Pathways of Influence of the Northern Hemisphere Mid-high Latitudes on East Asian Climate: A Review, Adv. Atmos. Sci., 36, 902–921, https://doi.org/10.1007/s00376-019-8236-5, 2019.

Li, J., Carlson, B. E., Yung, Y. L., Lv, D., Hansen, J., Penner, J. E., Liao, H., Ramaswamy, V., Kahn, R. A., Zhang, P., Dubovik, O., Ding, A. J., Lacis, A. A., Zhang, L., and Dong, Y. M.: Scattering and absorbing aerosols in the climate system, Nat. Rev.-Earth Environ., 3, 363–379, https://doi.org/10.1038/s43017-022-00296-7, 2022.

Li, Y., Xu, F. L., Feng, J., Du, M. Y., Song, W. J., Li, C., and Zhao, W. J.: Influence of the previous North Atlantic Oscillation (NAO) on the spring dust aerosols over North China, Atmos. Chem. Phys., 23, 6021–6042, https://doi.org/10.5194/acp-23-6021-2023, 2023.

Liu, X. D., Yin, Z., Zhang, X. Y., and Yang, X. C.: Analyses of the spring dust storm frequency of northern China in relation to antecedent and concurrent wind, precipitation, vegetation, and soil moisture conditions, J. Geophys. Res.-Atmos., 109, 2004JD004615, https://doi.org/10.1029/2004JD004615, 2004.

López-Parages, J., Rodríguez-Fonseca, B., and Terray, L.: A mechanism for the multidecadal modulation of ENSO teleconnection with Europe, Clim. Dyn., 45, 867–880, https://doi.org/10.1007/s00382-014-2319-x, 2015.

Lou, S. J., Russell, L. M., Yang, Y., Xu, L., Lamjiri, M. A., DeFlorio, M. J., Miller, A. J., Ghan, S. J., Liu, Y., and Singh, B.: Impacts of the East Asian Monsoon on springtime dust concentrations over China, J. Geophys. Res.-Atmos., 121, 8137–8152, https://doi.org/10.1002/2016JD024758, 2016.

Lou, S. J., Russell, L. M., Yang, Y., Liu, Y., Singh, B., and Ghan, S. J.: Impacts of interactive dust and its direct radiative forcing on interannual variations of temperature and precipitation in winter over East Asia, J. Geophys. Res.-Atmos., 122, 8761–8780, https://doi.org/10.1002/2017JD027267, 2017.

McPhaden, M. J. and Zhang, X. B.: Asymmetry in zonal phase propagation of ENSO sea surface temperature anomalies, Geophys. Res. Lett., 36, 2009GL038774, https://doi.org/10.1029/2009GL038774, 2009.

Najibi, N., Devineni, N., and Lall, U.: Compound Continental Risk of Multiple Extreme Floods in the United States. Geophys. Res. Lett., 50, e2023GL105297. https://doi.org/10.1029/2023GL105297, 2023.

Pan, L. L.: Observed positive feedback between the NAO and the North Atlantic SSTA tripole, Geophys. Res. Lett., 32, 2005GL022427, https://doi.org/10.1029/2005GL022427, 2005.

Parry, S., Lavers, D., Wilby, R., Prudhomme, C., Wood, P., Murphy, C., and O'Connor, P.: Abrupt drought termination in the British–Irish Isles driven by high atmospheric vapour transport, Environ. Res. Lett., 18, 104050, https://doi.org/10.1088/1748-9326/acf145, 2023.

Prospero, J. M., Nees, R. T., and Uematsu, M.: Deposition rate of particulate and dissolved aluminum derived from saharan dust in precipitation at Miami, Florida, J. Geophys. Res.-Atmos., 92, 14723–14731, https://doi.org/10.1029/JD092iD12p14723, 1987.

Rayner, N. A., Parker, D. E., Horton, E. B., Folland, C. K., Alexander, L. V., Rowell, D. P., Kent, E. C., and Kaplan, A.: Global analyses of sea surface temperature, sea ice, and night marine air temperature since the late nineteenth century, J. Geophys. Res.-Atmos., 108, 2002JD002670, https://doi.org/10.1029/2002JD002670, 2003.

Song, L. Y., Chen, S. F., Chen, W., Guo, J. P., Cheng, C. L., and Wang, Y.: Distinct evolutions of haze pollution from winter to following spring over the North China Plain: Role of the North Atlantic sea surface temperature anomalies. Atmos. Chem. Phys., 22, 1669–1688, https://doi.org/10.5194/acp-22-1669-2022, 2022.

Su, J. Z., Zhang, R. H., Li, T., Rong, X. Y., Kug, J., and Hong, C.: Causes of the El Niño and La Niña Amplitude Asymmetry in the Equatorial Eastern Pacific, J. Climate, 23, 605–617, https://doi.org/10.1175/2009JCLI2894.1, 2010.

Sung, M., Lim, G., and Kug, J.: Phase asymmetric downstream development of the North Atlantic Oscillation and its impact on the East Asian winter monsoon, J. Geophys. Res.-Atmos., 115, 2009JD013153, https://doi.org/10.1029/2009JD013153, 2010.

Takaya, K. and Nakamura, H.: A Formulation of a Phase-Independent Wave-Activity Flux for Stationary and Migratory Quasigeostrophic Eddies on a Zonally Varying Basic Flow, J. Atmospheric Sci., 58, 608–627, https://doi.org/10.1175/1520-0469(2001)058<0608:AFOAPI>2.0.CO;2, 2001.

Trenberth, K. E.: The Definition of El Niño, B. Am. Meteorol. Soc., 78, 2771–2777, https://doi.org/10.1175/1520-0477(1997)078<2771:TDOENO>2.0.CO;2, 1997.

Wallace, J. M. and Gutzler, D. S.: Teleconnections in the Geopotential Height Field during the Northern Hemisphere Winter, Mon. Weather Rev., 109, 784–812, https://doi.org/10.1175/1520-0493(1981)109<0784:TITGHF>2.0.CO;2, 1981.

Wang, B., Wu, R. G., and Fu, X. H.: Pacific–East Asian Teleconnection: How Does ENSO Affect East Asian Climate?, J. Climate, 13, 1517–1536, https://doi.org/10.1175/1520-0442(2000)013<1517:PEATHD>2.0.CO;2, 2000.

Wang, C., Ren, B. H., Li, G., Zheng, J. Q., Jiang, L. W., and Xu, D.: An Interdecadal Change in the Influence of the NAO on Atlantic-Induced Arctic Daily Warming around the Mid-1980s, Adv. Atmos. Sci., 40, 1285–1297, https://doi.org/10.1007/s00376-022-2218-8, 2023.

Wang, L., and Ting, M. F.: Stratosphere-Troposphere Coupling Leading to Extended Seasonal Predictability of Summer North Atlantic Oscillation and Boreal Climate, Geophys. Res. Lett., 49, e2021GL096362. https://doi.org/10.1029/2021GL096362, 2022.

Wang, T. H., Tang, J. Y., Sun, M. X., Liu, X. W., Huang, Y. X., Huang, J. P., Han, Y., Cheng, Y. F., Huang, Z. W., and Li, J. M.: Identifying a transport mechanism of dust aerosols over South Asia to the Tibetan Plateau: A case study, Sci. Total Environ., 758, 11, https://doi.org/10.1016/j.scitotenv.2020.143714, 2021.

Wang, Z. Q., Yang, S., Lau, N.-C., and Duan, A. M.: Teleconnection between Summer NAO and East China Rainfall Variations: A Bridge Effect of the Tibetan Plateau, J. Climate, 31, 6433–6444, https://doi.org/10.1175/JCLI-D-17-0413.1, 2018.

Woollings, T., Franzke, C., Hodson, D. L. R., Dong, B., Barnes, E. A., Raible, C. C., and Pinto, J. G.: Contrasting interannual and multidecadal NAO variability, Clim. Dyn., 45, 539–556, https://doi.org/10.1007/s00382-014-2237-y, 2015.

Wu, B., Zhou, T. J., and Li, T.: Atmospheric Dynamic and Thermodynamic Processes Driving the Western North Pacific Anomalous Anticyclone during El Niño. Part I: Maintenance Mechanisms, J. Climate, 30, 9621–9635, https://doi.org/10.1175/JCLI-D-16-0489.1, 2017.

Wu, J., Kurosaki, Y., Shinoda, M., and Kai, K.: Regional Characteristics of Recent Dust Occurrence and Its Controlling Factors in East Asia, Sola, 12, 187–191, https://doi.org/10.2151/sola.2016-038, 2016.

Wu, R. G. and Chen, S. F.: What Leads to Persisting Surface Air Temperature Anomalies from Winter to Following Spring over Mid- to High-Latitude Eurasia? J. Climate, 33, 5861–5883, https://doi.org/10.1175/JCLI-D-19-0819.1, 2020.

Wu, Z. W., Wang, B., Li, J. P., and Jin, F. F.: An empirical seasonal prediction model of the east Asian summer monsoon using ENSO and NAO, J. Geophys. Res.-Atmos., 114, 2009JD011733, https://doi.org/10.1029/2009JD011733, 2009.

Wu, Z. W., Li, J. P., Jiang, Z. H., He, J. H., and Zhu, X. Y.: Possible effects of the North Atlantic Oscillation on the strengthening relationship between the East Asian Summer monsoon and ENSO, Int. J. Climatol., 32, 794–800, https://doi.org/10.1002/joc.2309, 2012.

Xi, X. and Sokolik, I. N.: Dust interannual variability and trend in Central Asia from 2000 to 2014 and their climatic linkages, J. Geophys. Res.-Atmos., 120, https://doi.org/10.1002/2015JD024092, 2015.

Yang, Y., Zeng, L. Y., Wang, H. L., Wang, P. Y., and Liao, H.: Dust pollution in China affected by different spatial and temporal types of El Niño, Atmos. Chem. Phys., 22, 14489–14502, https://doi.org/10.5194/acp-22-14489-2022, 2022.

Yao, W. R., Gui, K., Wang, Y. Q., Che, H. Z., and Zhang, X. Y.: Identifying the dominant local factors of 2000–2019 changes in dust loading over East Asia, Sci. Total Environ., 777, 146064, https://doi.org/10.1016/j.scitotenv.2021.146064, 2021.

Yu, Y., Notaro, M., Liu, Z. Y., Wang, F. Y., Alkolibi, F., Fadda, E., and Bakhrjy, F.: Climatic controls on the interannual to decadal variability in Saudi Arabian dust activity: Toward the development of a seasonal dust prediction model, J. Geophys. Res.-Atmos., 120, 1739–1758, https://doi.org/10.1002/2014JD022611, 2015.

Zhang, P., Wu, Z. W., and Jin, R.: How can the winter North Atlantic Oscillation influence the early summer precipitation in Northeast Asia: effect of the Arctic sea ice, Clim. Dyn., 56, 1989–2005, https://doi.org/10.1007/s00382-020-05570-2, 2021a.

Zhang, R. H., Li, T. R., Wen, M., and Liu, L. K.: Role of intraseasonal oscillation in asymmetric impacts of El Niño and La Niña on the rainfall over southern China in boreal winter, Clim. Dyn., 45, 559–567, https://doi.org/10.1007/s00382-014-2207-4, 2015.

Zhang, R. H., Tian, W. S., He, X., Qie, K., Liu, D., and Tian, H. Y.: Enhanced influence of ENSO on winter precipitation over southern China in recent decades, J. Climate, 1–36, https://doi.org/10.1175/JCLI-D-21-0182.1, 2021b.

Zhang, W. J., Li, J. P., and Jin, F. F.: Spatial and temporal features of ENSO meridional scales, Geophys. Res. Lett., 36, 2009GL038672, https://doi.org/10.1029/2009GL038672, 2009.

Zhang, W. J., Li, H. Y., Stuecker, M. F., Jin, F. F., and Turner, A. G.: A New Understanding of El Niño's Impact over East Asia: Dominance of the ENSO Combination Mode, J. Climate, 29, 4347–4359, https://doi.org/10.1175/JCLI-D-15-0104.1, 2016.

Zhang, X. Y., Gong, S. L., Zhao, T. L., Arimoto, R., Wang, Y. Q., and Zhou, Z. J.: Sources of Asian dust and role of climate change versus desertification in Asian dust emission, Geophys. Res. Lett., 30, 2003GL018206, https://doi.org/10.1029/2003GL018206, 2003.

Zhao, C. F., Yang, Y. K., Fan, H., Huang, J. P., Fu, Y. F., Zhang, X. Y., Kang, S. C., Cong, Z. Y., Letu, H., and Menenti, M.: Aerosol characteristics and impacts on weather and climate over the Tibetan Plateau, Natl. Sci. Rev., 7, 492–495, https://doi.org/10.1093/nsr/nwz184, 2020.

Zhao, S., Li, J. P., and Sun, C.: Decadal variability in the occurrence of wintertime haze in central eastern China tied to the Pacific Decadal Oscillation, Sci. Rep., 6, 27424, https://doi.org/10.1038/srep27424, 2016.

Zhao, Y., Huang, A. N., Zhu, X. S., Zhou, Y., and Huang, Y.: The impact of the winter North Atlantic Oscillation on the frequency of spring dust storms over Tarim Basin in northwest China in the past half-century, Environ. Res. Lett., 8, 024026, https://doi.org/10.1088/1748-9326/8/2/024026, 2013.

Zheng, F., Li, J. P., Li, Y. J., Zhao, S., and Deng, D. F.: Influence of the Summer NAO on the Spring-NAO-Based Predictability of the East Asian Summer Monsoon, J. Appl. Meteorol. Clim., 55, 1459–1476, https://doi.org/10.1175/JAMC-D-15-0199.1, 2016a.

Zheng, Y., Zhao, T. L., Che, H. Z., Liu, Y., Han, Y. X., Liu, C., Xiong, J., Liu, J. H., and Zhou, Y. K.: A 20-year simulated climatology of global dust aerosol deposition, Sci. Total Environ., 557–558, 861–868, https://doi.org/10.1016/j.scitotenv.2016.03.086, 2016b.

Zhou, F., Shi, J., Liu, M. H., and Ren, H. C.: Linkage between the NAO and Siberian high events on the intraseasonal timescale, Atmos. Res., 281, 106478, https://doi.org/10.1016/j.atmosres.2022.106478, 2023.

Zhu, C. W., Wang, B., and Qian, W. H.: Why do dust storms decrease in northern China concurrently with the recent global warming? Geophys. Res. Lett., 35, 2008GL034886, https://doi.org/10.1029/2008GL034886, 2008.

Zuo, J. Q., Ren, H. L., Li, W. J., and Wang, L.: Interdecadal Variations in the Relationship between the Winter North Atlantic Oscillation and Temperature in South-Central China, J. Climate, 29, 7477–7493, https://doi.org/10.1175/JCLI-D-15-0873.1, 2016.